Electronic Supplementary Material (ESI) for Dalton Transactions.

Triphenylamine substituted copper and zinc phthalocyanines as alternative hole-transporting materials for solution processed perovskite solar cells

SUPPORTING INFORMATION

Gizem Gümüşgöz Çelik,[a] Ayşe Nur Şahin,[b] Ferruh Lafzi,[c] Nurullah Saraçoğlu,[c] Ahmet Altındal,*[b] Ayşe Gül Gürek,*[a] Devrim Atilla*[a]

[a] *Department of Chemistry, Faculty of Fundamental Sciences, Gebze Technical University, 41400, Gebze, Kocaeli, Turkey*

[b] *Department of Physics, Yıldız Technical University, 34220, Esenler, Istanbul, Turkey*

[c] *Department of Chemistry, Faculty of Sciences, Atatürk University, Erzurum 25240, Turkey*

Table of Contents

1. Synthesis of TPA derivatives

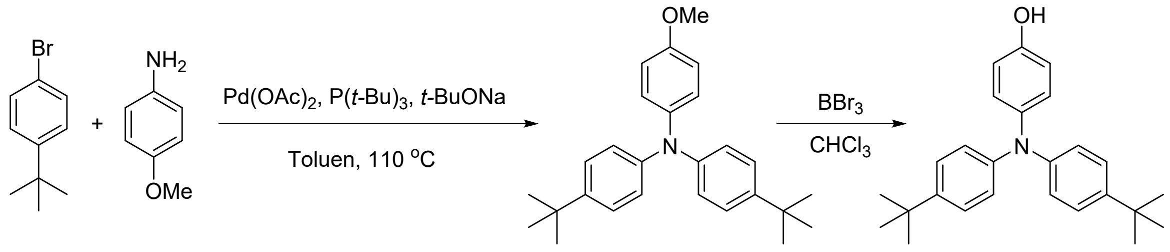

1 **2** **3** **4**

4-(*tert*-Butyl)-*N*-(4-(*tert*-butyl)phenyl)-*N*-(4-methoxyphenyl)aniline (3)

To a solution of **1** (*p*-anisidine, 1.0 g, 8.12 mmol) in toluene (30 mL), **2** (1-bromo-4-*tert*-butylbenzene, 3.52 mL, 20.3 mmol) and *t*-BuONa (2.34 g, 24.3 mmol) was added. The system was purged with nitrogen several times. Then, P(*t*-Bu)$_3$ (394 mg, 1.95 mmol) and Pd(OAc)$_2$ (218 mg, 0.97 mmol) were added to the mixture, and the solution was heated to reflux overnight. After cooling to room temperature, the resulting mixture was quenched by water, extracted with ethyl acetate (3 × 20 mL), and then dried over Na_2SO_4. The crude product was purified by column chromatography on silica gel (petroleum ether/ethyl acetate = 99:1 v/v) to afford 4-(*tert*-butyl)-*N*-(4-(*tert*-butyl)phenyl)-*N*-(4-methoxyphenyl)aniline (**3**) as a white solid (2.3 g, 73%; mp: 142.3-143.3 °C). **^{1}H NMR (400 MHz, CDCl$_3$) δ ppm:** 7.30 – 7.25 (m, AA' part of AA'BB' system, =CH, 4H), 7.15 – 7.11 (m, AA' part of AA'BB' system, =CH, 2H), 7.04 – 7.00 (m, BB' part of AA'BB' system, =CH, 4H), 6.90 – 6.86 (m, BB' part of AA'BB' system, =CH, 2H), 3.84 (s, CH_3, 3H), 1.36 (s, CH_3, 18H). **^{13}C NMR (100 MHz, CDCl$_3$) δ ppm:** 155.8, 145.7, 144.4, 141.2, 127.0, 125.9, 122.4, 114.7, 55.5, 34.2, 31.5.

4-(Bis(4-(*tert*-butyl)phenyl)amino)phenol (4)

To a solution of 4-(*tert*-butyl)-*N*-(4-(*tert*-butyl)phenyl)-*N*-(4-methoxyphenyl)aniline (2.0 g, 5.16 mmol) in $CHCl_3$ (30 mL) at 0 °C, a solution of BBr_3 (1.74 mL, 18.1 mmol) in $CHCl_3$ (10 mL) was added slowly with dropping funnel under stirring. After stirring for 1 h at this temperature, the reaction mixture was allowed to warm to room temperature and stirred for an additional 24 h. The reaction was carefully quenched with NH_4Cl solution using an ice bath and the resulting solution was washed with water (2 × 30 mL), dried over Na_2SO_4, and evaporated to afford compound **4** as a white solid (1.7 g, 88%; mp: 177.5-178.5 °C). **^{1}H NMR (400 MHz, DMSO-*d$_6$*) δ ppm:** 9.34 (bs, OH, 1H), 7.23 – 7.19 (m, AA' part of AA'BB' system, =CH, 4H), 6.89 – 6.85 (m, AA' part of AA'BB' system, =CH, 2H), 6.83 – 6.79 (m, BB' part of AA'BB' system, =CH, 4H), 6.75 – 6.71 (m, BB' part of AA'BB' system, =CH, 2H), 1.24 (s, CH_3, 18H). **^{13}C NMR (100 MHz, DMSO-*d$_6$*) δ ppm:** 154.1, 145.4, 143.5, 138.5, 127.4, 125.8, 121.5, 116.2, 33.8, 31.2.

2. Spectra of synthesized compounds

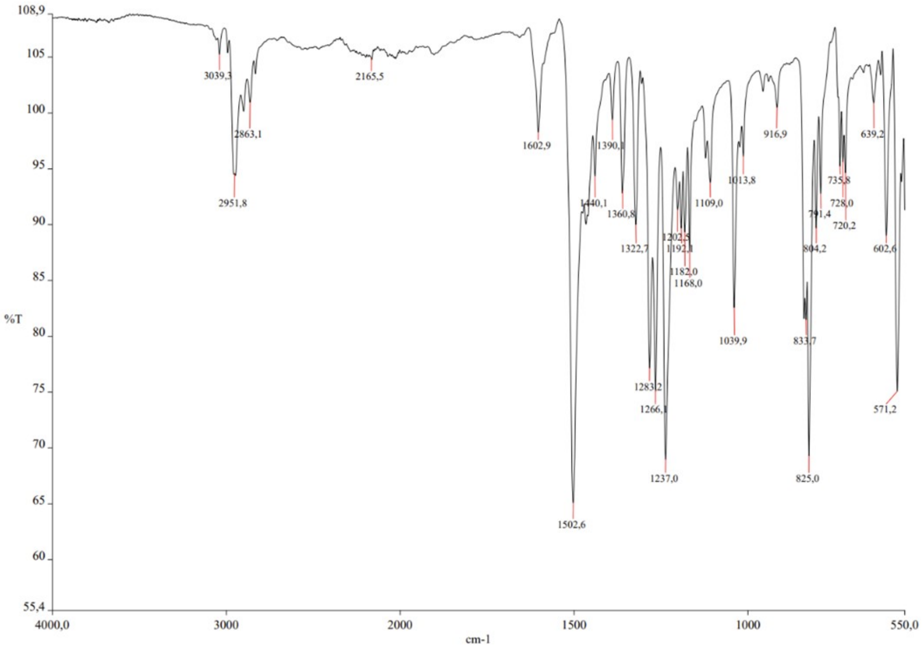

Figure S1. FT-IR spectrum of **3**

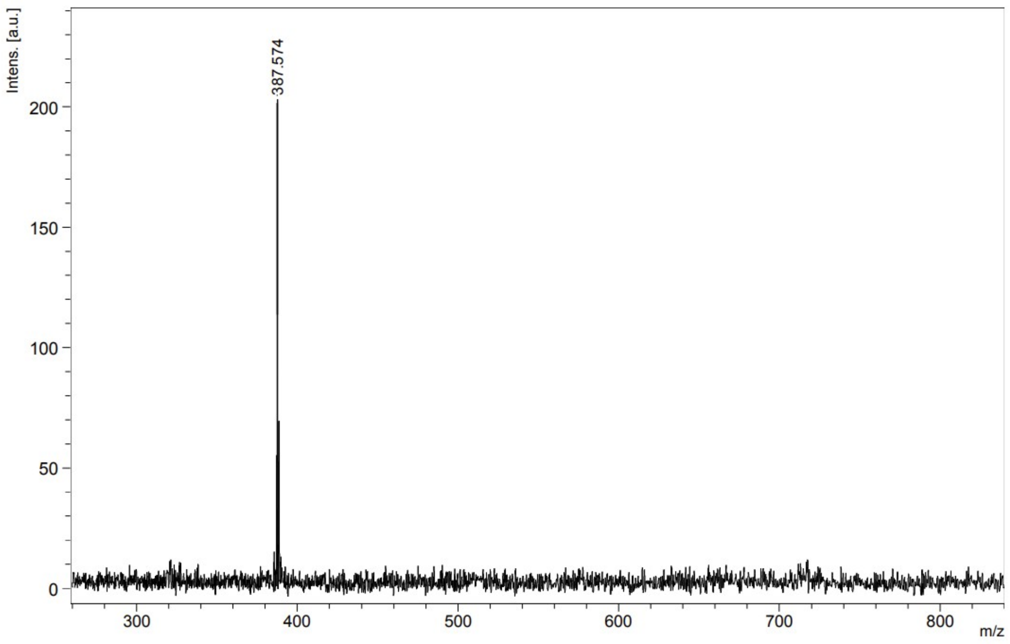

Figure S2. MALDI-TOF MS spectrum of **3**

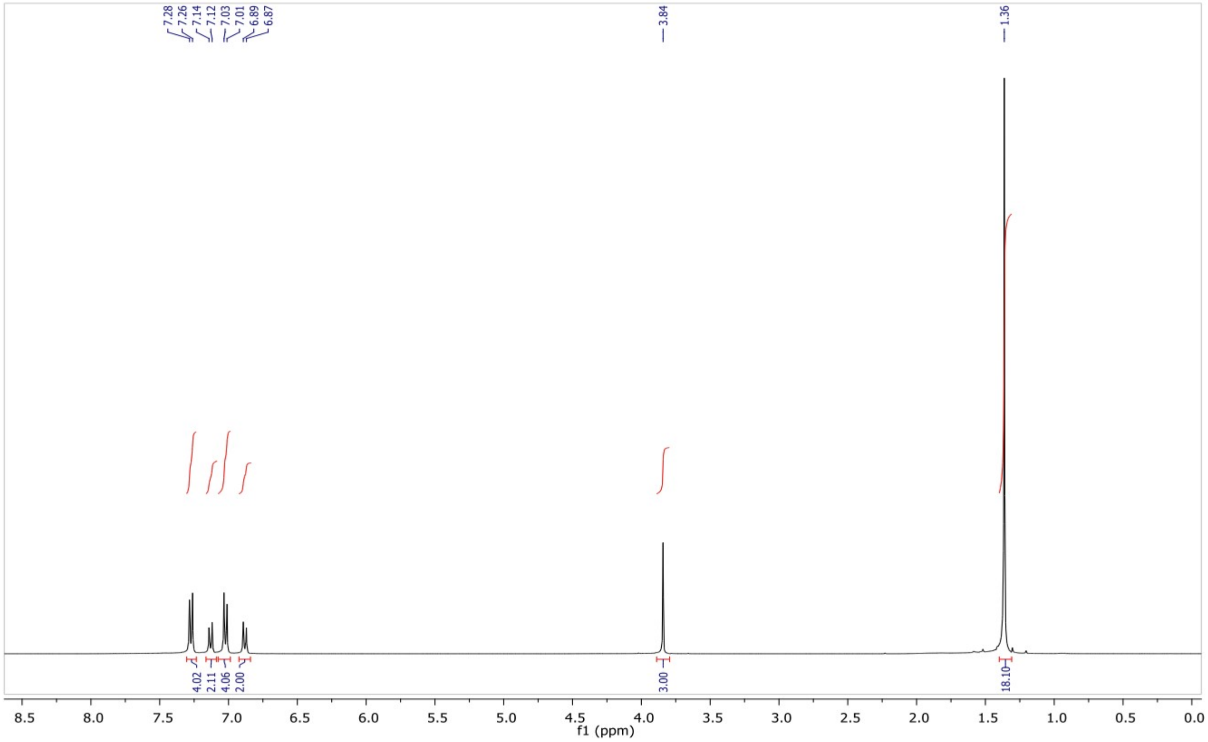

Figure S3. ^{1}H-NMR spectrum of **3**

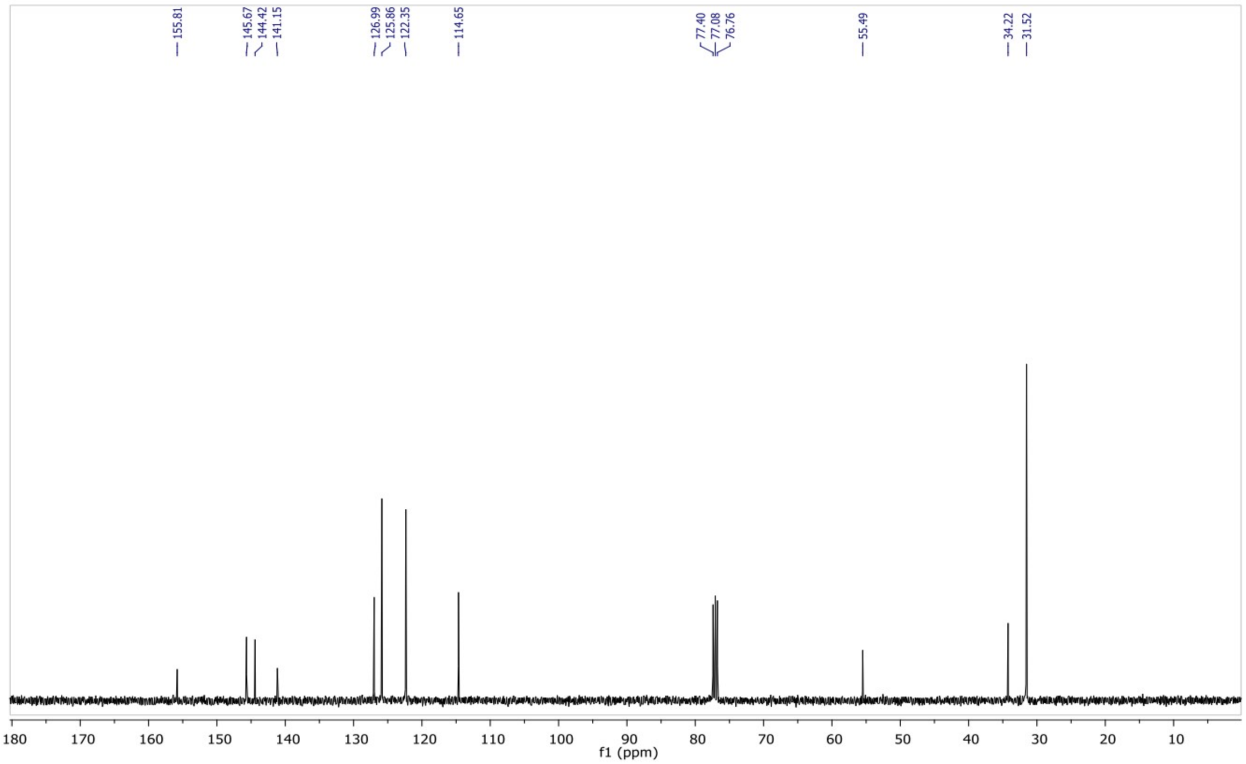

Figure S4. ^{13}C-NMR spectrum of **3**

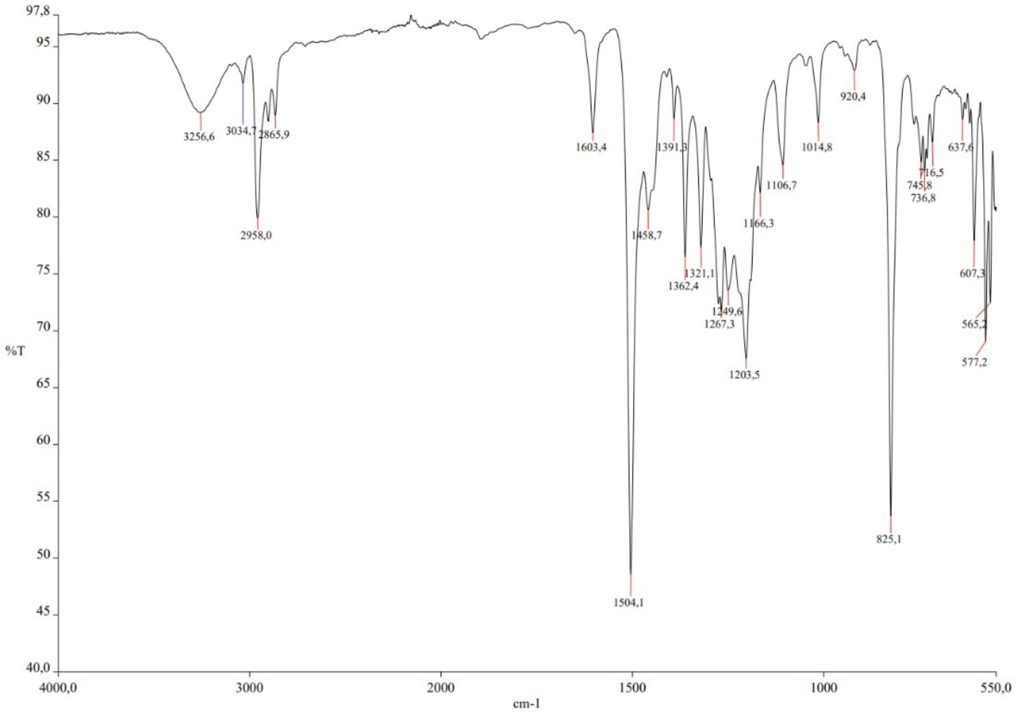

Figure S5. FT-IR spectrum of **4**

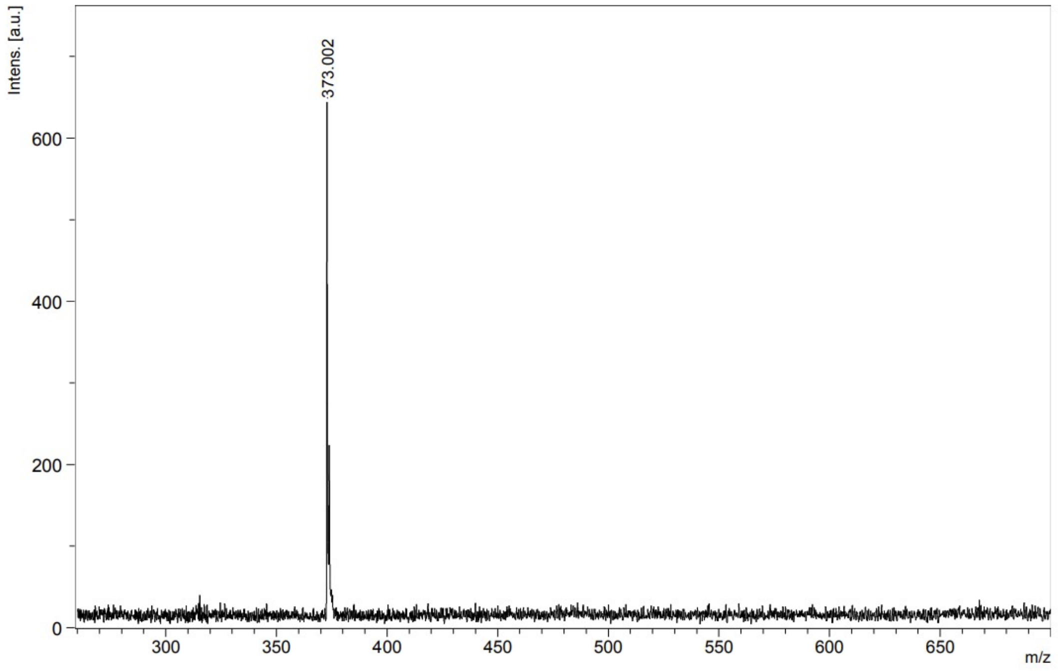

Figure S6. MALDI-TOF MS spectrum of **4**

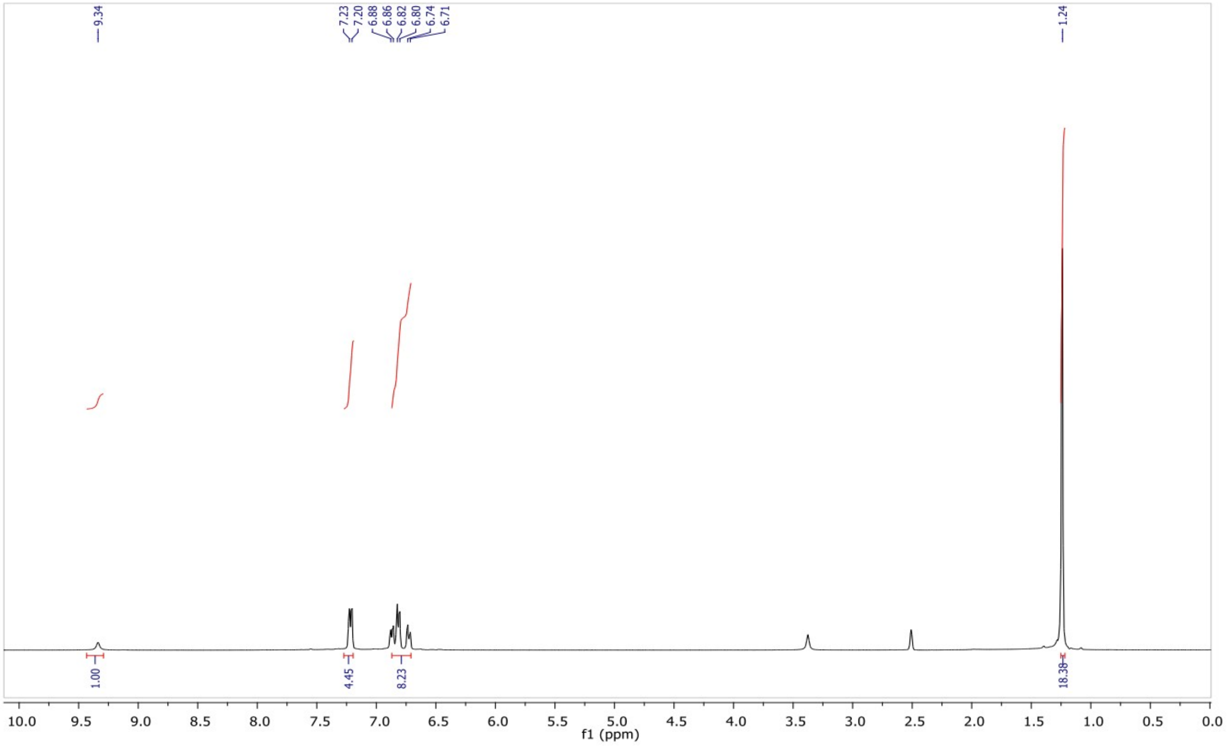

Figure S7. ^{1}H-NMR spectrum of **4**

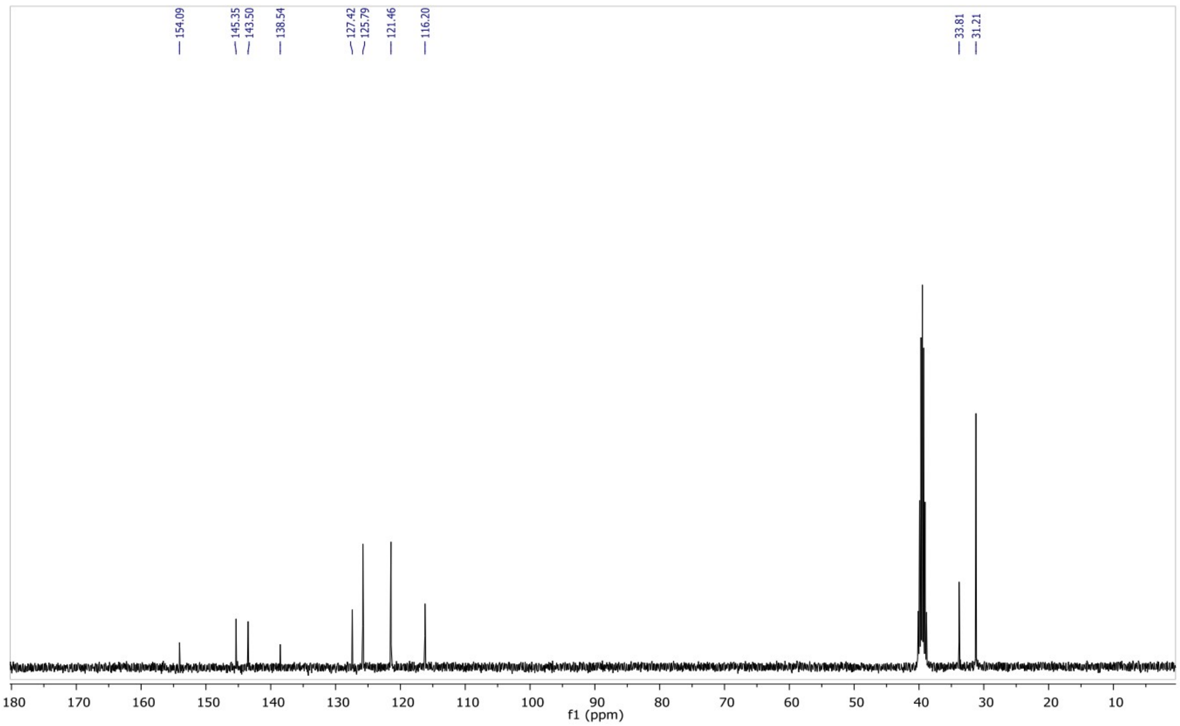

Figure S8. ^{13}C-NMR spectrum of **4**

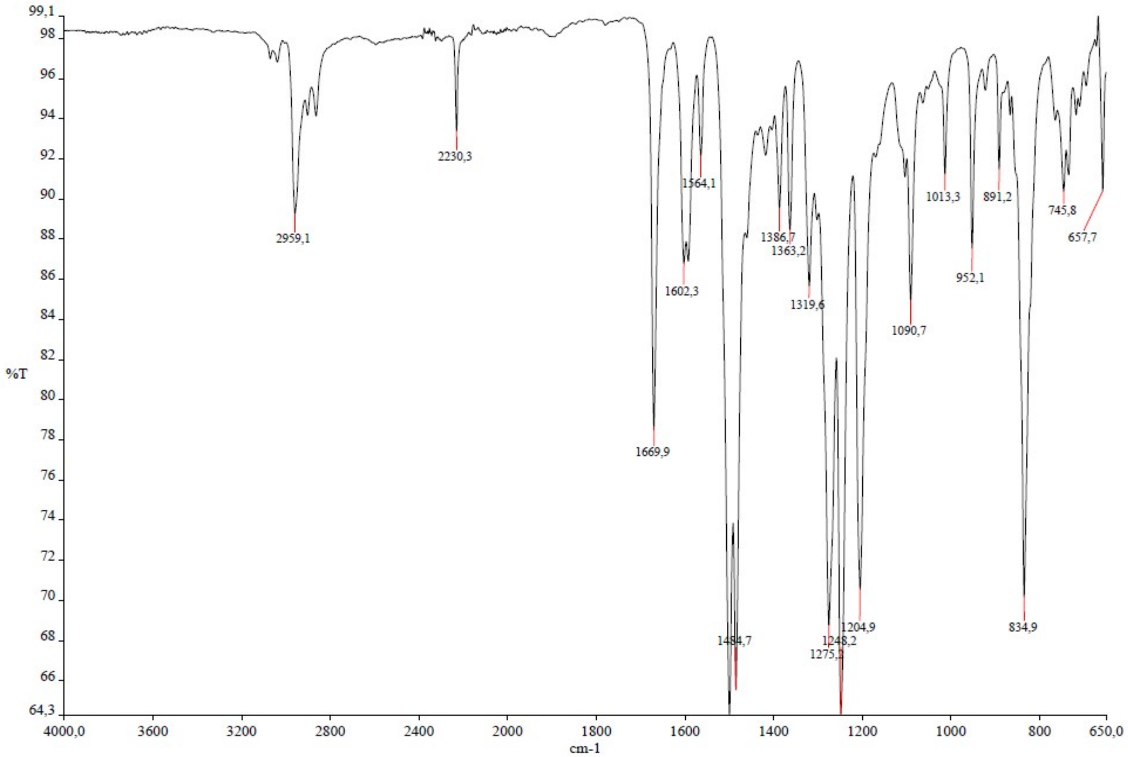

Figure S9. FT-IR spectrum of **PN**

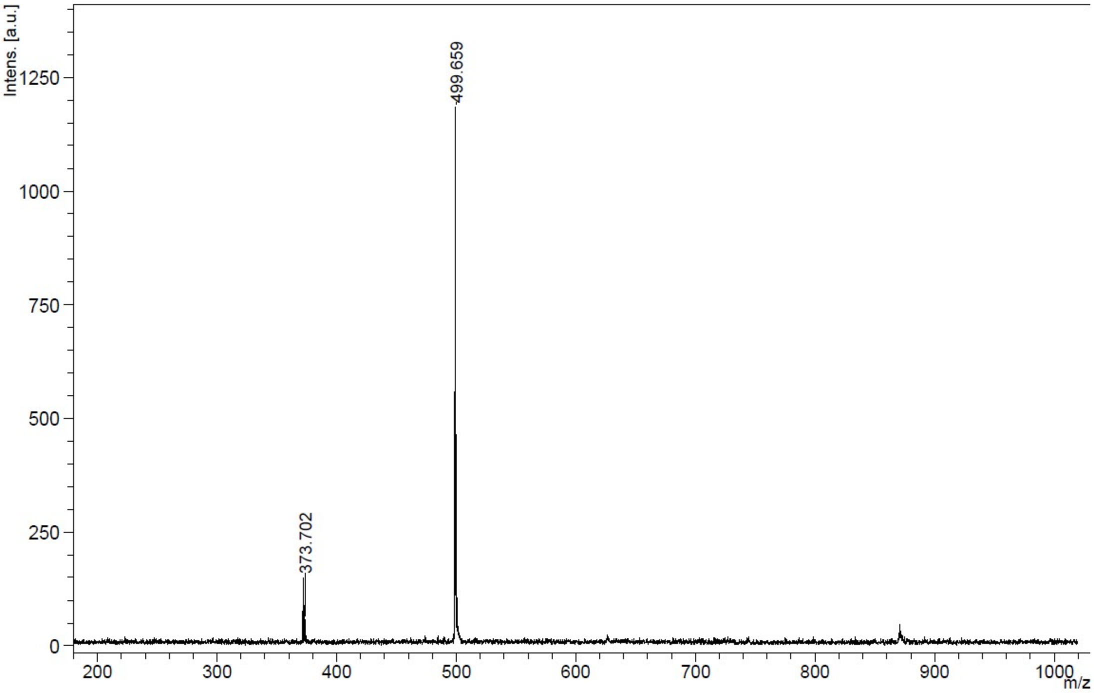

Figure S10. MALDI-TOF MS spectrum of **PN**

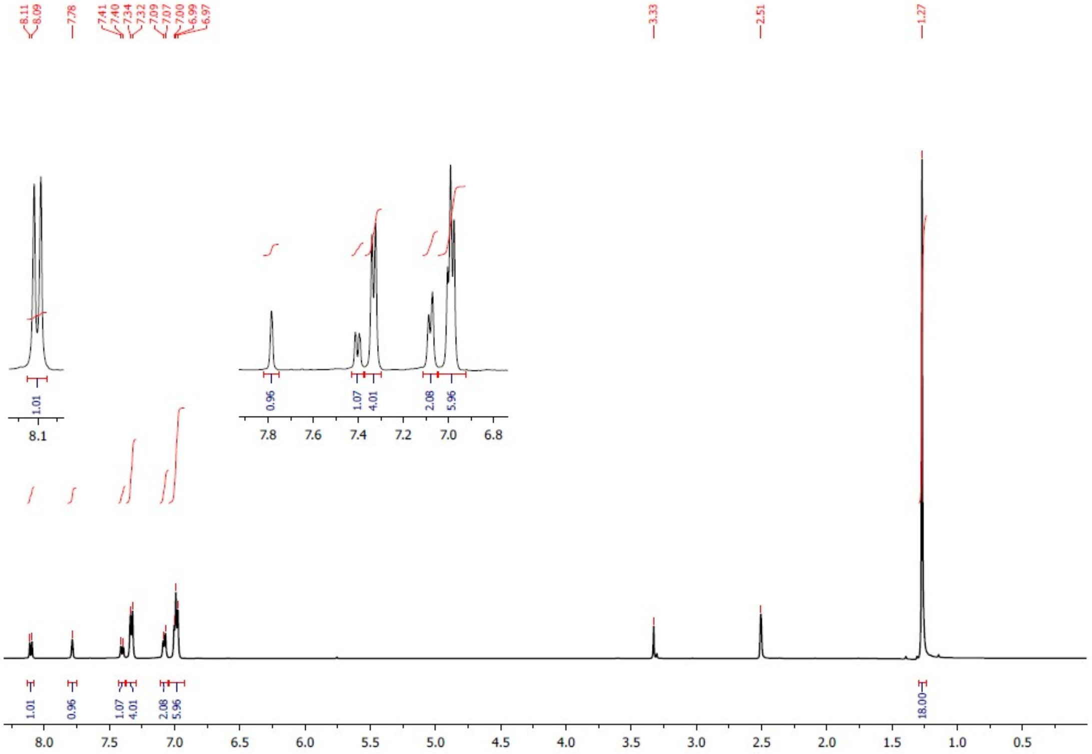

Figure S11. ^{1}H NMR spectrum of **PN**

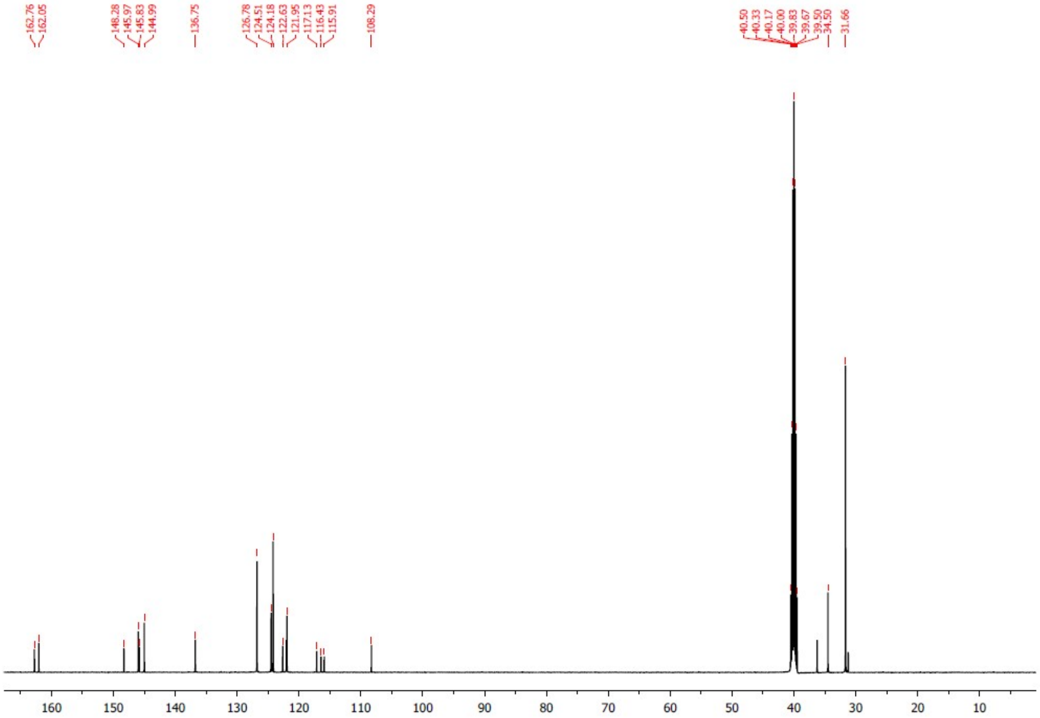

Figure S12. ^{13}C NMR spectrum of **PN**

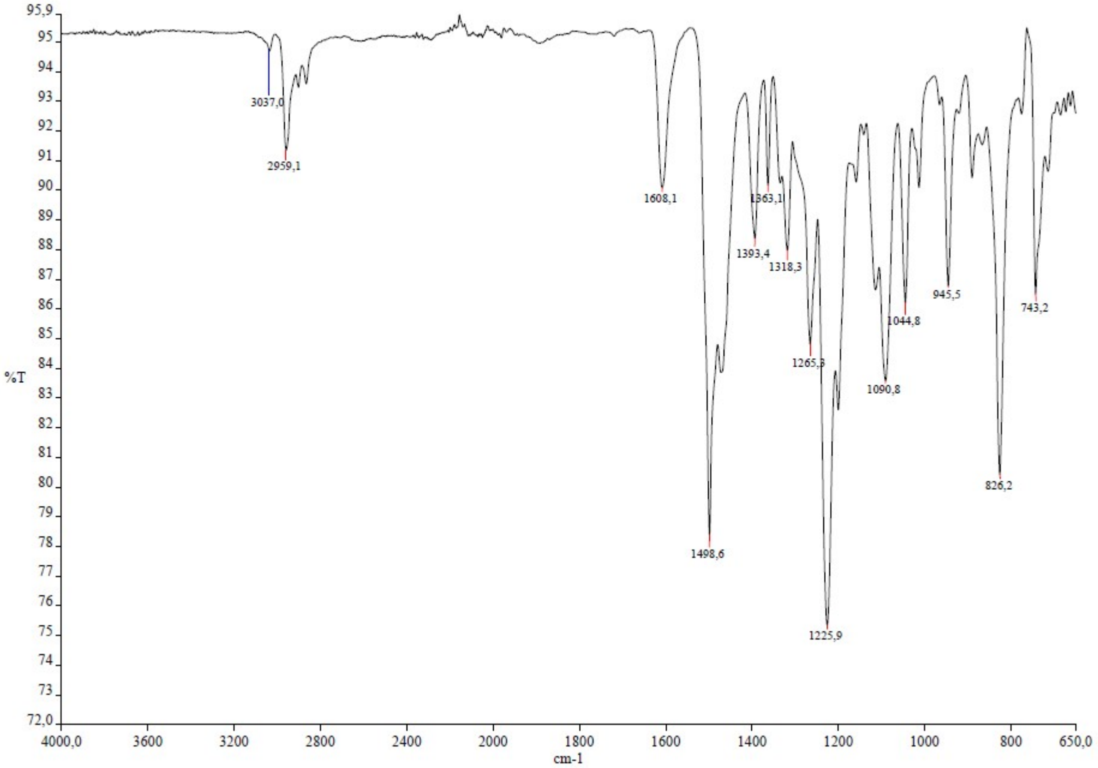

Figure S13. FT-IR spectrum of **p-ZnPc**

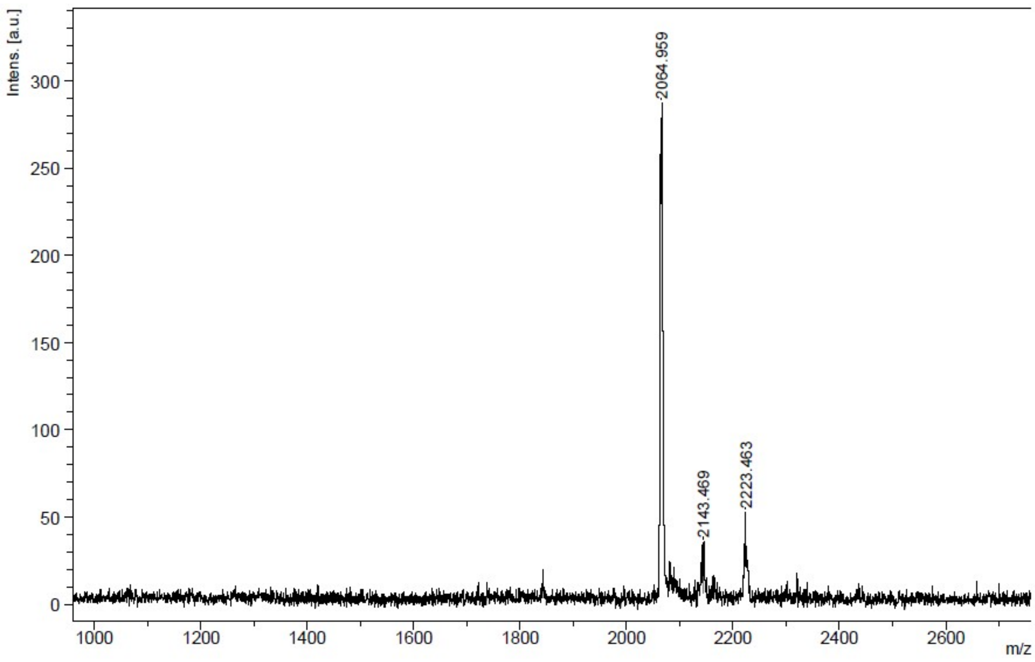

Figure S14. MALDI-TOF MS spectrum of **p-ZnPc**

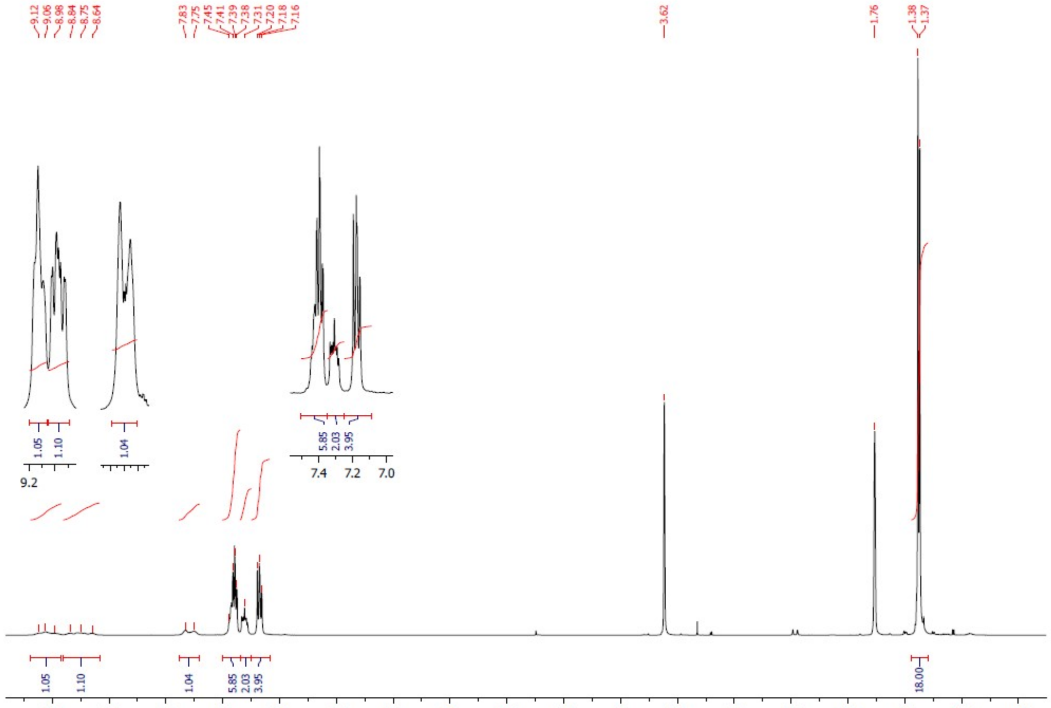

Figure S15. ^{1}H-NMR spectrum of **p-ZnPc**

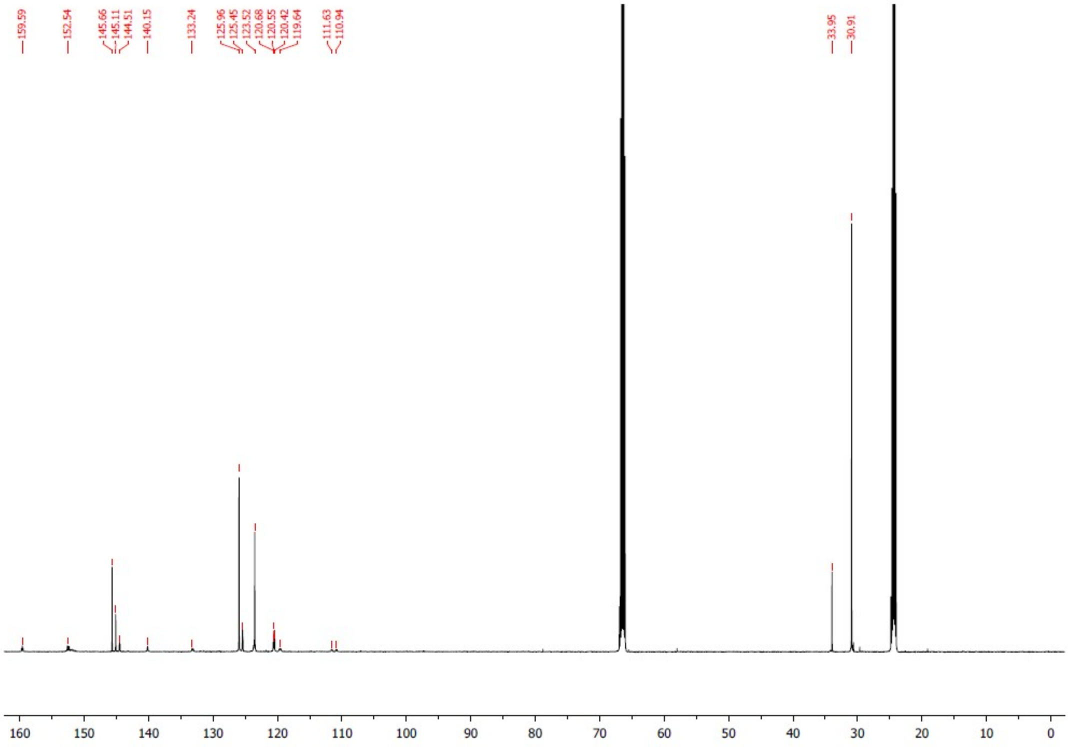

Figure S16. ^{13}C NMR spectrum of **p-ZnPc**

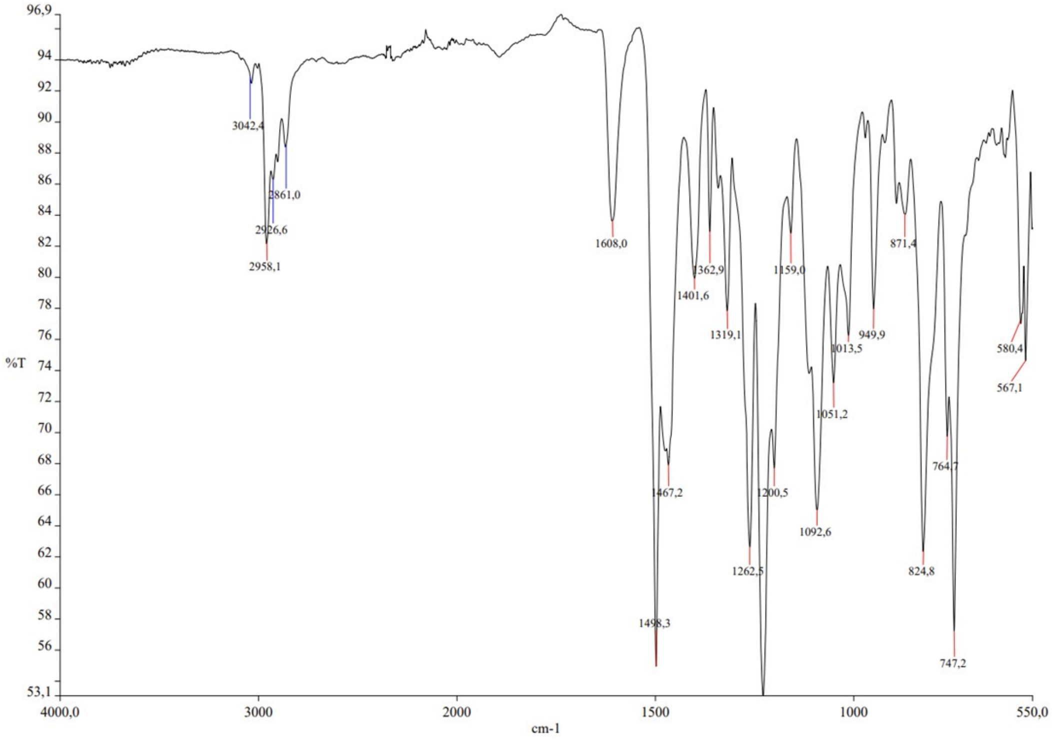

Figure S17. FT-IR spectrum of **p-CuPc**

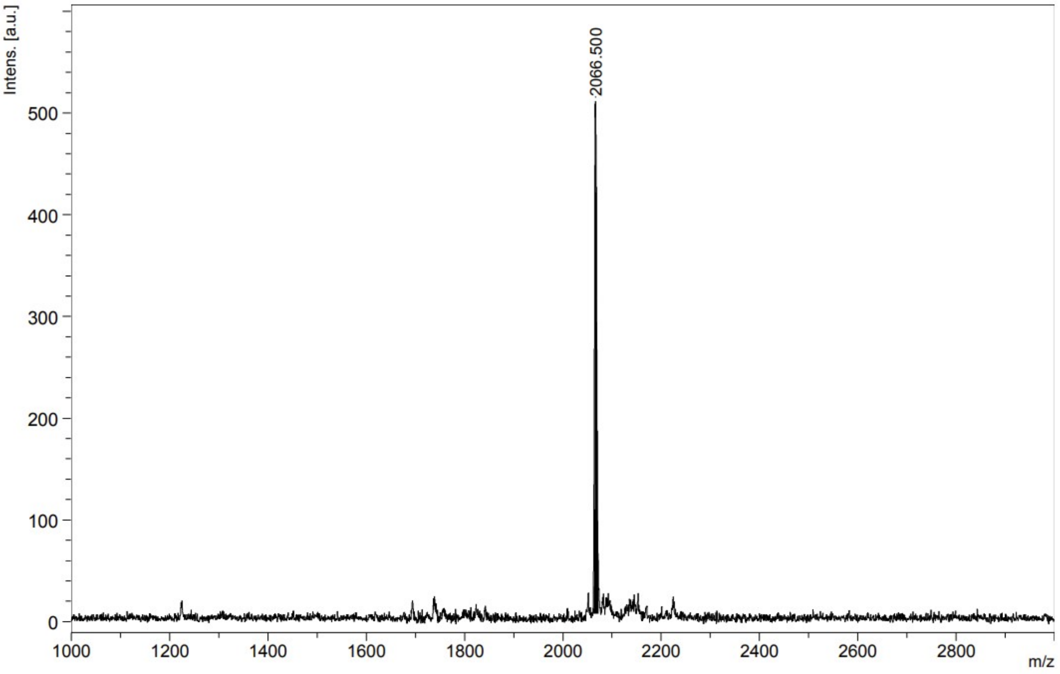

Figure S18. MALDI-TOF MS spectrum of **p-CuPc**

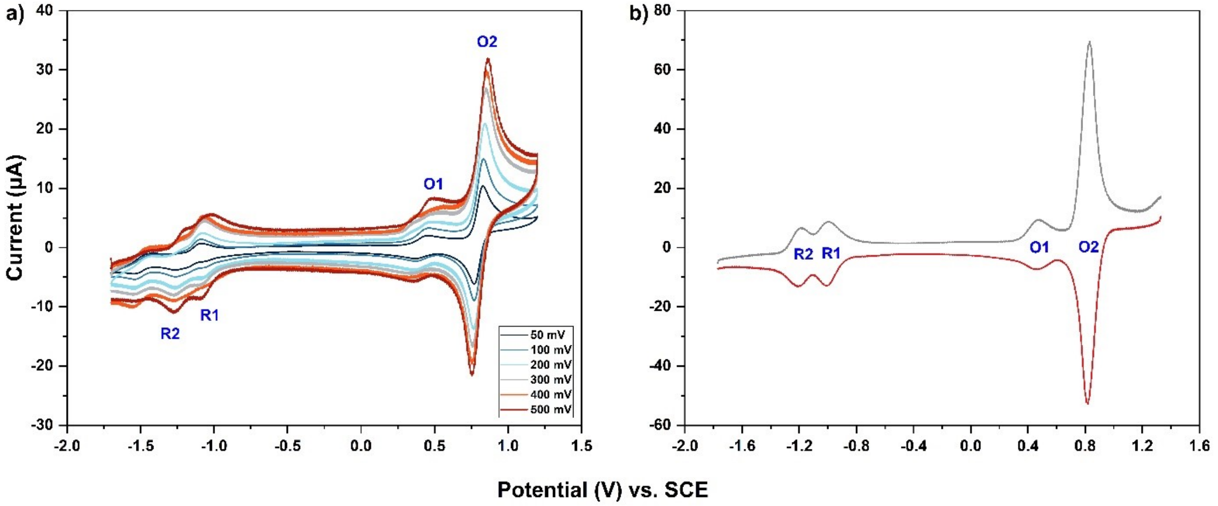

Figure S19. a) CV of **p-ZnPc** at various scan rates on Pt in DCM containing 0.1 M NBu_4PF_6. b) SWV of **p-ZnPc** (pulse size: 100 mV; step size: 5 mV; frequency: 25 Hz.)

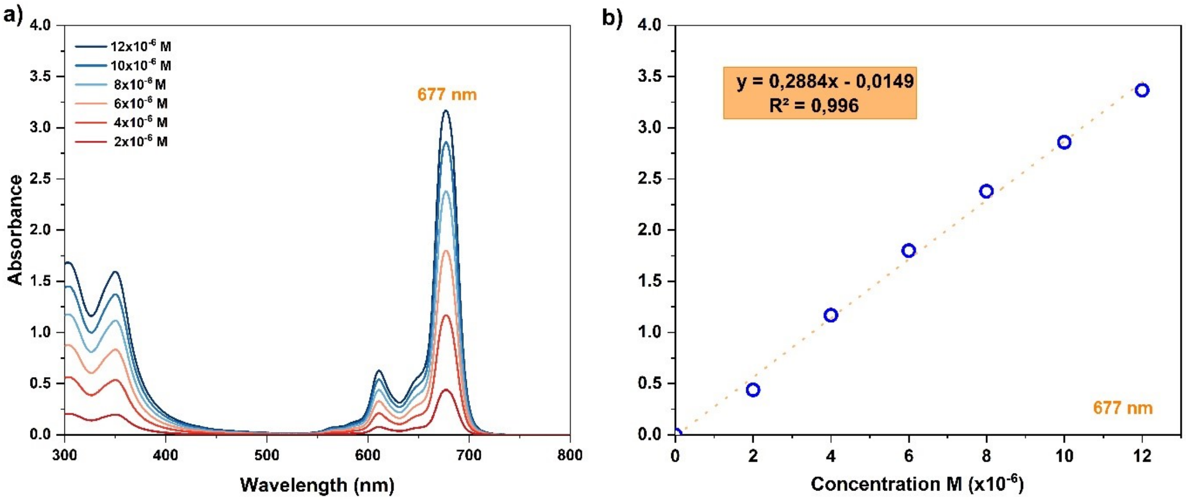

Figure S20. UV-Vis spectra of **p-ZnPc,** a) different concentration in THF (**λ_{maks}=677 nm**), b) Absorbance-concentration graph for maximum absorption (ε=2.9x10^5 Lmol^{-1} cm^{-1}, logε= 5.46)

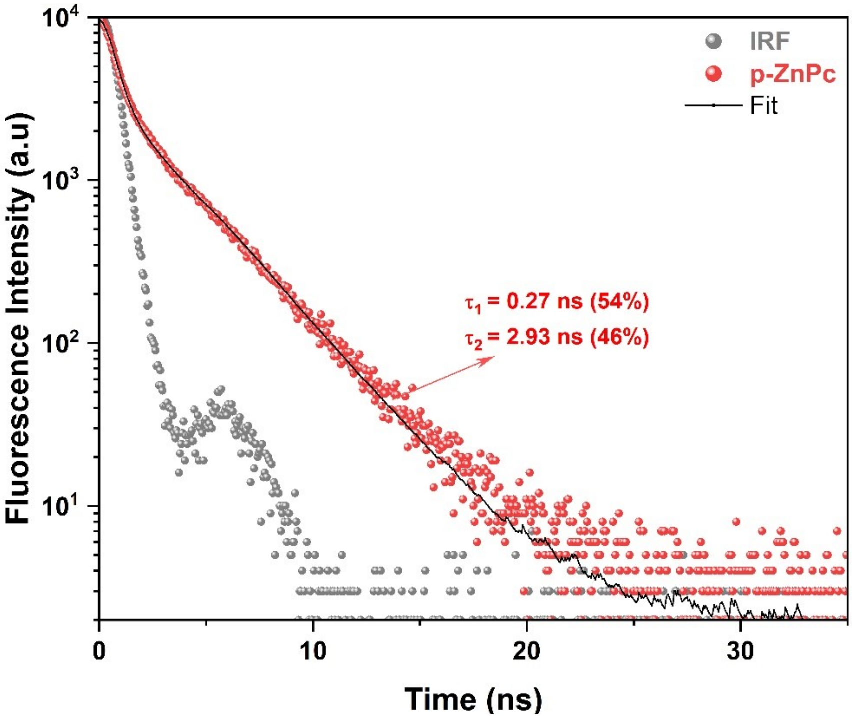

Figure S21. Fluorescence decay curves of **p-ZnPc** in THF (NanoLed λ_{ex} :674nm).

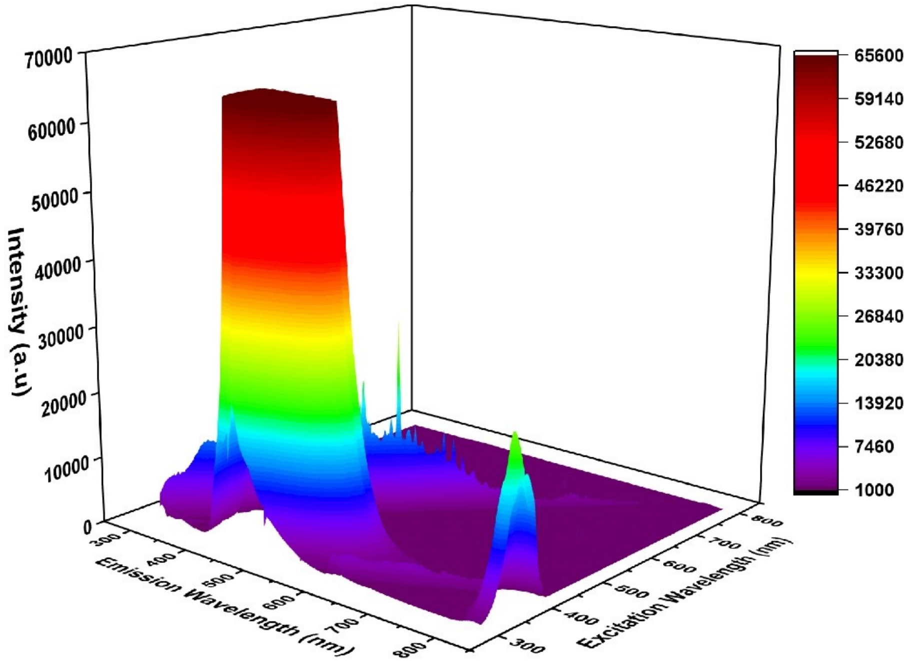

Figure S22. 3D- EMM (Excitation/Emission Matrix) spectra of **p-ZnPc** in THF.

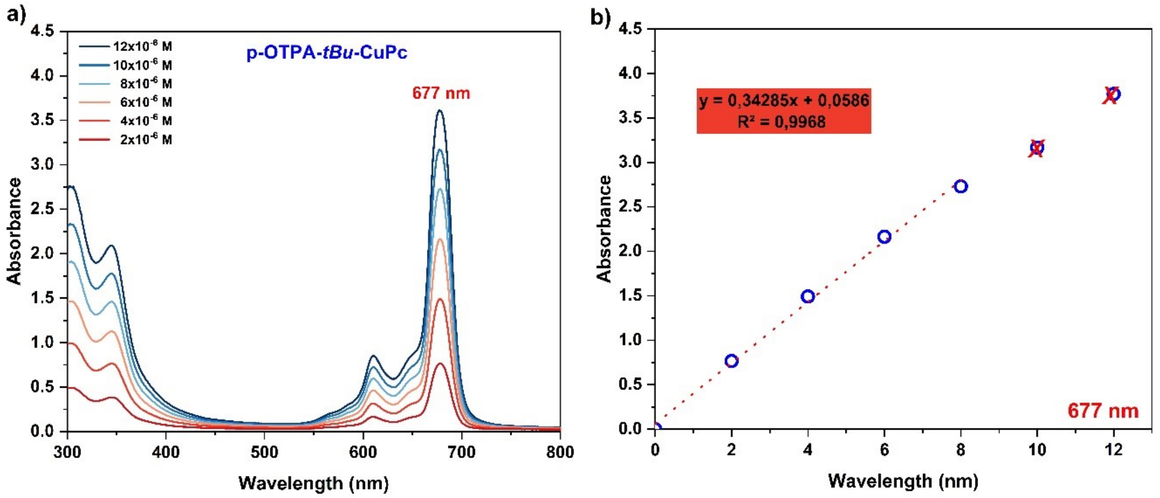

Figure S23. UV-Vis spectra of **p-CuPc,** a) different concentration in THF (**λ_{maks}=677 nm**), b) Absorbance-concentration graph for maximum absorption (**ε**=3.4x10^5 Lmol^{-1}cm^{-1}, **log ε**= 5.53)

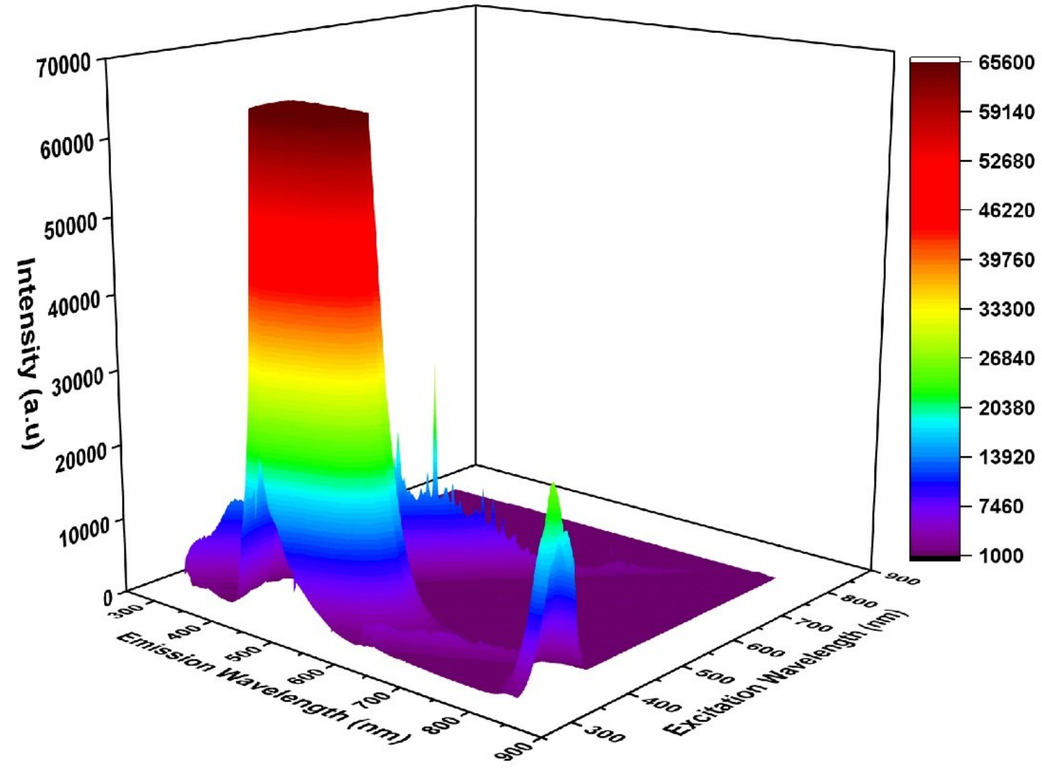

Figure S24. 3D EMM spectra of **p-CuPc** in THF.

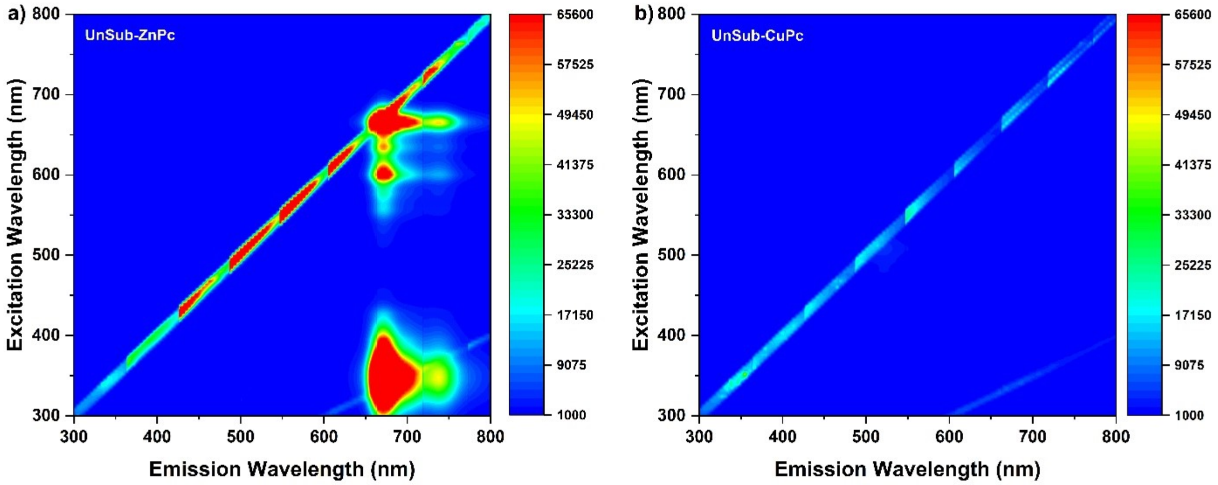

Figure S25. 3D excitation/emission matrix contour plots of unsubstituted Pc derivatives in THF a) **UnSubZnPc,** b) **UnSubCuPc**

3. Photophysical measurements

Flouresence Quantum Yield Calculation

In order to evaluate the photophysical properties of **p-ZnPc** and **p-CuPc**, fluorescence quantum yields (Φ_F) were determined using a comparative method (eqn (1)) where a solution of unsubstituted ZnPc ($\Phi_F = 0.25$) in THF was used as a standard[1].

$$\Phi_F = \Phi_{F_{Std}} \frac{F \,.\, A_{Std}\, \eta^2}{F_{Std}\, \eta_{Std}^2} \qquad \text{(Eq. 1)}$$

In this equation, F, Fstd, A, and Astd represent the fluorescence bands areas and absorbance values at the excitation wavelength for the sample and standard.

Time-correlated single-photon counting fluorescence measurements were performed to directly determine the fluorescence lifetime of compound **p-ZnPc** and **p-CuPc** with appropriate calculation

Solid-state bandgap measurement by diffuse reflectance spectra (DRS)

The energy required to excite an electron from the valence band to the conduction band is defined as the bandgap, which is essential in investigating semiconductors' photophysical and photochemical properties. The equation proposed by Tauc[2] in 1966 and developed with the contributions of Davis and Mott[3] is given as equation 2.

$$(\alpha.h\nu)^{1/\gamma} = A\,(h\nu - E_g) \qquad \text{Eq. 2}$$

where h: Planck's constant, ν: frequency of photons α: energy-dependent absorption coefficient, E_g: solid-state bandgap, A: constant. The ɣ factor depends on the electron transition and equals 1/2 or 2 at the direct and indirect transition bandgap, respectively[4].

The solid-state band gap energy is often determined by diffuse reflectance spectra (DRS). Firstly, the measured DRS spectra were converted into absorption spectra by applying the Kubelka-Munk function given in equation 2.

$$F(R_\infty) = \frac{K}{S} = \frac{(1 - R_\infty)}{2R_\infty} \qquad \text{Eq. 3}$$

where K: absorption coefficient, S scattering coefficient, $R_\infty=R_{sample}/R_{standard}$, represents the reflection of an infinitely thick sample. The Tauc plot final equation obtained by putting $F(R_\infty)$ instead of theα value given in equation 1 is given below as equation 3.

$$\left(F(R_\infty).\,h\nu\right)^{1/ɣ} = A\,(h\nu - E_g) \qquad \text{Eq. 4}$$

The spectra were recorded using a UV−vis spectrophotometer (UV-2600 Shimadzu) equipped with an integrated sphere attachment and a powder sample holder. The collected R∞(λ) spectra were transformed according to eqs 2 and the direct allowed transition, the value of the ɣ is used as 1/2.

References

1 E. T. Saka, M. Durmuş and H. Kantekin, *J. Organomet. Chem.*, 2021, ***696*****(4)**, 913-924.

2 J. Tauc, in *Amorphous and Liquid Semiconductors*, Springer US, 1974, pp. 159–220.

3 E. A. Davis and N. F. Mott, *Philos. Mag.*, 1970, **22**, 903–922.

4 P. Makuła, M. Pacia, and W. Macyk, *J. Phys. Chem. Lett.,* 2018, **9(23)**, 6814-6817.